Aramide et al., *Cogent Engineering* (2019), 6: 1584938
https://doi.org/10.1080/23311916.2019.1584938

cogent engineering

MATERIALS ENGINEERING | RESEARCH ARTICLE

Studies on the combined effects of titania and silicon carbide on the phase developments and properties of carbon-clay based ceramic composite

Fatai Olufemi Aramide[1,2*], O. D. Adepoju[1], Adeolu Adesoji Adediran[3] and Abimbola Patricia Popoola[2]

Received: 24 September 2018
Accepted: 17 February 2019
First Published: 21 February 2019

*Corresponding author: Fatai Olufemi Aramide, Mechanical Engineering, Landmark University, Nigeria
E-mail: foaramide@futa.edu.ng; aramidefo@tut.ac.za

Reviewing editor:
Blaza Stojanovic, Faculty of Engineering, University of Kragujevac, Serbia

Additional information is available at the end of the article

Abstract: Effects of titania (TiO_2) and silicon carbide (SiC) on phase development and physico-mechanical properties of mullite-carbon were investigated. Powdered clay, kaolinite and graphite of predetermined compositions were blended with additives using ball mill for 3 h at 60 rev/min. Samples were produced by uniaxial compression and sintered between 1400°C and 1600°C for 1 h. They were characterized for various properties, phases developed and microstructural features. The addition of TiO_2 and SiC in the sample lead to the formation of TiC in the sample at 1400°C and 1600°C. This takes place through high-temperature solid-state reaction (reaction sintering) of TiO_2 and SiC. This also contributes to the reduction in the apparent porosity of the sample with increased sintering temperature. The presence of titania in the sample does not favour the stability of anorthite beyond 1400°C. The formation of 50.6% mullite in the sample at 1500°C made it have the highest

Fatai Olufemi Aramide

ABOUT THE AUTHORS

Fatai Olufemi Aramide is a senior faculty member of the Metallurgical and Materials Engineering, Federal University of Technology, Akure, Nigeria. His research focus on ceramic Engineering. He also has interests in metal matrix composite, light metal/alloys and laser cladding related research. Currently, he is a NRF-TWAS postdoctoral fellow at the Department of Chemical, Metallurgical and Materials Engineering, Tshwane University of Technology, Pretoria, South Africa.

O. D. Adepoju is a graduate student being supervised by Dr Fatai O. Aramide.

Adeolu Adesoji Adediran is a Lecturer in the Department of Mechanical Engineering, Landmark University, Omu-Aran, Kwara State, Nigeria.

Abimbola Patricia Popoola is a professor of Metallurgical Engineering in the Department of Chemical, Metallurgical and Materials Engineering, Tshwane University of Technology, Pretoria, South Africa. She is the leader of Advanced Engineering Materials and Surface Technologies research group. She has mentored a sizable number of graduate students both at masters and doctoral levels.

PUBLIC INTEREST STATEMENTS

Large deposit of clay materials is found in specific locations across the world. These materials, are used for several Engineering application. Nigeria is not an exception in the committee of nations having a large deposit of clay. The manuscript reports on the effect of titania (TiO_2) and silicon carbide (SiC) additives on the properties and phase development in mullite-carbon ceramic composites produced from graphite, clay sourced from Ifon in Nigeria and Okpella kaolin. It reports on how the ceramic samples become toughened both by the in-situ formation of mullite and titanium carbide with the matrix of the ceramic. This leads to an improvement in the mechanical properties of the samples.

cold crushing strength and absorbed energy. Young's modulus of the sample increased with increased sintering temperature. The sample sintered at 1500°C is considered optimum.

Subjects: Aerospace Engineering; Tribology; Vibration; Manufacturing Engineering; Materials Science; Production Engineering

Keywords: Additives; ceramic composite; carbon-clay; phase development; mullite

1. Introduction

Composites are engineering materials having a combination of two or more constituents whether organic, inorganic or any metal which will give the combined properties of each phase (Jayasankar et al., 2010).

Ceramic matrix composites (CMCs) are very useful materials applicable in the area of demanding mechanical and thermal requirements. Although ceramic matrices are prone to brittle failure, CMCs have been developed to achieve quasi-ductile fracture behaviour and maintain all other advantages of monolithic ceramics at high temperatures. For instance, CMCs can be designed to be as strong as metals, while they are much lighter and with the ability to withstand much higher temperatures. These advantages led to their application in automotive and aerospace engineering (Silvestre, Silvestre, & de Brito, 2015). There are several factors upon which the properties of CMC depend, such as the quantity, distribution of the final formed and the processing route used for the synthesis. The raw materials and inclusion additives into the CMC have a great influence on phase evolution in the material and final property of the product (Elgamouz & Tijani, 2018). Many researchers have focussed research activities in this direction; trying to improve on the properties of existing CMC or developing new CMC of better service properties. Badiee et al. (Badiee, Ebadzadeh, & Golestani-Fard, 2001) studied the effects of CaO, MgO, TiO_2 and ZrO_2 on the mullitization process in Iranian andalusite located in Hamedan mines. They discovered that all, but ZrO_2 favour the formation of mullite from andalusite.

Ebadzadeh and Ghasemi (Ebadzadeh & Ghasemi, 2002) produced zirconia mullite composites from α-alumina, aluminium nitrate, zircon powder with TiO_2 additive. Aramide et al. (Aramide, Alaneme, Olubambi, & Borode, 2014) synthesized mullite-yttria stabilized zirconia composites. Chandra et al. (Chandra, Das, Sengupta, & Maitra, 2013) synthesized zirconia-toughened ceramics with a mullite matrix based on the quaternary system ZrO_2–Al_2O_3–SiO_2–TiO_2 in the temperature range 1450–1550°C using zircon-alumina-titania mixtures. Aramide and Popoola (Aramide & Popoola, 2017) investigated the effects of niobium oxide additive on phase development and physico-mechanical properties of zirconia-clay based ceramic composite. They discovered that niobium oxide additive inhibits mullite formation in preference to aluminium niobate and sillimanite.

The lead author in collaboration with other researchers have reported various findings on the effects of titania and silicon carbide of phase development and properties of mullite-carbon ceramic composites (Aramide & Akintunde, 2017a, 2017b; Aramide, Akintunde, & Oyetunji, 2016; Aramide, Akintunde, & Popoola, 2017). But they observed that the investigated samples were characterized with poor mechanical properties. The main aim of this work is to improve on the mechanical properties of the carbon-based ceramic composites through the addition of Ifon clay.

2. Experimental

2.1. Materials

The kaolin sample was sourced from Okpella, Edo State, (of geographical location 7. 27′ 21° N, 6. 34′ 65°) Nigeria. The clay used was sourced from Ifon, Ondo State, (6. 55′ 0′ N, 5. 46° 0′ E) Nigeria

Table 1. Constitution of the various samples

Sample designation	Graphite (wt.%)	Kaolin (wt.%)	Ifon Clay (wt.%)	SiC (wt.%)	TiO_2 (wt.%)
D	30	35	25	5	5

and graphite was sourced from (Pascal Chemicals, Akure). The Ifon clay and kaolin samples were first separately soaked in water for 3 days to dissolve the deleterious materials in them and at the same time to form a slurry. The slurries were then sieved to remove deleterious materials and other foreign substances. The sieved slurries were then allowed to settle down for 3 days after which the clear floating water was decanted. The dispersed fine clays in water (clay slurries) were then poured into plaster of Paris (POP) moulds and left undisturbed for 3 days in order to allow the remaining water present to drain out completely. The resulting plastic clay masses were sun dried and subsequently dried in a laboratory oven at 110°C for 24 h. The resulting dried clay samples were crushed and milled in a Rawwley Sussex grinder to an average particle size of 300 µm. The mass per cent of the composition was computed using Equations (1–2), by computing the densities of the various constituents and the individual powders volume fraction in each composition. The powders were weighed per batch of 100,.00 g on a sensitive electronic weighing balance to five (5) decimal places. The individual (batch) composition was thoroughly mixed in a ball mill for 3 h at 60 rev/min. The compositions of the blended samples are shown in Table 1.

If

$$M_t = V_k\rho_k + V_C\rho_C + V_{Ifon}\rho_{Ifon} + V_{SiC}\rho_{SiC} + V_{TiO_2}\rho_{TiO_2}, \quad (1)$$

where

V_k, V_C, V_{Ifon}, V_{SiC} and V_{TiO2} are, respectively, the volume fraction of kaolin, graphite, Ifon clay, SiC and TiO_2. $\rho_{k,}$ ρ_C, ρ_{Ifon}, ρ_{SiC} and ρ_{TiO2} are, respectively, the density of kaolin, graphite, Ifon clay, SiC and TiO_2. M_t is the total mass contribution of all the components. And if M is the mass of each batch, then the mass contribution of each component could be calculated from:

$$M_c = \frac{V_c\rho_c \times M}{M_t}. \quad (2)$$

M_c is the mass contribution of a component in a batch (kaolin or graphite or Ifon clay or SiC or TiO_2), V_c, ρ_c the respective volume fraction and density of the component. The resulting homogenous powder mixtures were compacted uniaxially into standard sample dimensions for the various analyses. The moulded materials were fired at varying temperatures (1,400°C, 1,500°C and 1,600°C) in an electric furnace. The rate of firing differs with increased temperature (room temperature to 500°C the sintering rate was 250°C/min, 501°C to 1,000°C the sintering rate was 10°C/min while above 1,000°C the sintering rate was 3°C/min). On reaching the various sintering temperatures, the samples were held for 1 h at the temperature before the furnace was switched off and the samples were allowed to cool in the furnace. The samples were subjected to the various tests to examine the phase evolved during sintering and to evaluate how this affects their physical and mechanical properties.

2.2. Testing

2.2.1. Apparent porosity

Test samples from each of the ceramic composite samples were dried out for 12 h at 110°C. The dry weight of each fired sample was taken and recorded as D. Each sample was immersed in water for 6 h to soak and weighed while being suspended in air. The weight was recorded as *W*. Finally,

the specimen was weighed when immersed in water (Aramide, 2015; Aramide et al., 2017). This was recorded as *S*. The apparent porosity was then calculated from the expression:

$$\%\text{apparent porosity (AP)} = \frac{(W-D)}{(W-S)} \times 100. \tag{3}$$

2.2.2. Bulk density

The test specimens were dried out at 110°C for 12 h to ensure total water loss. Their dry weights were measured and recorded. They were allowed to cool and then immersed in a beaker of water. Bubbles were observed as the pores in the specimens were filled with water. Their soaked weights were measured and recorded. They were then suspended in a beaker one after the other using a thread, and their respective suspended weights were measured and recorded (Aramide, 2015; Aramide et al., 2017). Bulk densities of the samples were calculated using the relation:

$$\text{Bulk density (BD)} = \frac{D}{(W-S)}, \tag{4}$$

where *D* represents the weight of dried specimen, *S* represents the weight of dried specimen suspended in water and *W* represents the weight of soaked specimen in the air.

2.2.3. Water absorption

The test sample was dried out in an oven till a constant weight of the sample was obtained. The sample was then placed in a vessel containing water in order to be completely submerged without touching the bottom of the vessel in which it is suspended. The vessel was then heated slowly so that the water boiled after heating. After boiling for about an hour with the evaporated water replaced, the sample was allowed to cool at room temperature for 24 h. The sample was then renamed, blotted and then reweighed. The percentage of water absorption was calculated as shown:

$$\text{Water Absorption (WA)} = \frac{(\text{Soaked wt} - \text{Dried wt})}{(\text{Dried wt})} \times 100. \tag{5}$$

2.2.4. Cold compression strength, modulus of elasticity and absorbed energy

Cold compression strength test is to determine the compression strength to the failure of each sample, an indication of its probable performance under load. The standard ceramic samples were dried in an oven at a temperature of 110°C, allowed to cool. The cold compression strength tests were performed on INSTRON SERIES 3369 at a fixed crosshead speed of 10 mm min^{-1}. Samples were prepared according to (Aramide et al., 2017; Aramide, 2015, ASTM C133–97, 2015). Once the original dimension was imputed into the machine, it automatically calculates and displays the mechanical properties (compression strength, strain, Young's modulus and absorbed energy) on the display unit (screen). The cold crushing strength of standard and conditioned samples can be calculated from the equation:

$$\text{Cold Crushing Strength} = \frac{(\text{Load to fracture})}{(\text{Surface area of sample.})} \tag{6}$$

2.2.5. Qualitative and quantitative (XRD)

The samples were prepared for XRD analysis using a backloading preparation method. The samples were analysed using a PANalyticalX'Pert Pro powder diffractometer with X'Celerator detector and variable divergence- and receiving slits with Fe filtered Co-Kα radiation. The phases obtained were identified using Match! Software. Graphical representations of the qualitative result will then follow. The relative phase amounts in weight% were estimated using the Rietveld method (FullProf). Amorphous phases, present were not taken into consideration in the quantification.

2.2.6. Scanning electron microscopy

Morphology and microanalysis of the clay and composite samples were determined using ultra-high resolution field emission scanning electron microscope (UHR-FEGSEM) equipped with energy dispersive spectroscopy (EDS). The pulverize clay samples were graphite coated. The sintered samples were studied using UHR-FEGSEM equipped with EDS. Particle images are obtained with a secondary electron detector.

3. Results and discussion

Table 2 shows the phases developed in the various sintered samples, while Table 3 shows the physical with mechanical properties of the sintered. Figure 1 shows the x-ray diffraction pattern of the Ifon clay sample. From the figure, the major mineralogical phases are silica, aluminosilicate, haematite and titania. Figure 2 shows the phases in the samples sintered at various temperatures. Figure 3 to 8 show the effects of sintering temperature and additives on the physical and mechanical properties of the various samples. While Figure 9–11 show the secondary electron images, backscattered with energy dispersive spectroscopy (SEM/EDS) data of the samples sintered at various temperatures.

3.1. Combined effects of titania (TiO_2) and silicon carbide on the phases developed in the sample (sample D)

Table 2 and Figure 2 show the combined effects of titania, silicon carbide and sintering temperature on the phases developed in the samples D. From the figure and table, it is observed that at

Table 2. Showing the various phases developed in the samples

Sample	Graphite	TiO_2	SiC	Mullite	Anorthite	TiC	Quartz	Microcline	Cristobalite
DT1	4.6	9.4	0.0	15.6	18.0	13.7	5.0	29.4	4.3
DT2	3.8	7.8	0.7	50.6	0.0	0.8	0.7	12.9	0.0
DT3	29.0	0.0	15.3	10.3	0.0	6.8	5.3	28.9	0.4

Table 3. Showing the values of investigated physical and mechanical properties

Sample	Temp. (°C)	Stress (MPa)	Strain (mm/mm)	Impact (J)	Modulus E (MPa)	Bulk (g/cm^3)	WA (%)	AP (%)
D	1400	7.48136	0.08239	3.29092	90.8042	2.271	18.66	28.56
	1500	18.70020	0.11868	10.54072	157.5683	1.753	18.95	27.79
	1600	14.16836	0.07359	7.04267	192.5311	1.771	17.86	27.13

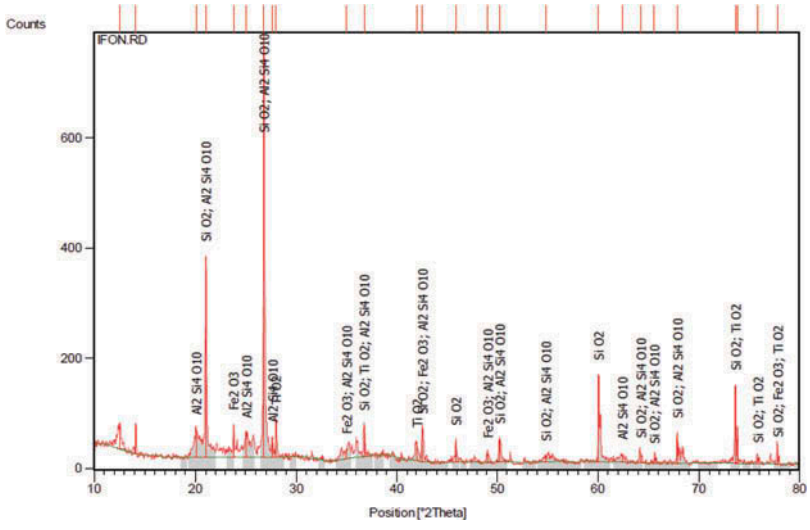

Figure 1. X-ray diffraction pattern (phase analysis) of Ifon clay sample.

Figure 2. Phases in samples D sintered at various temperatures.

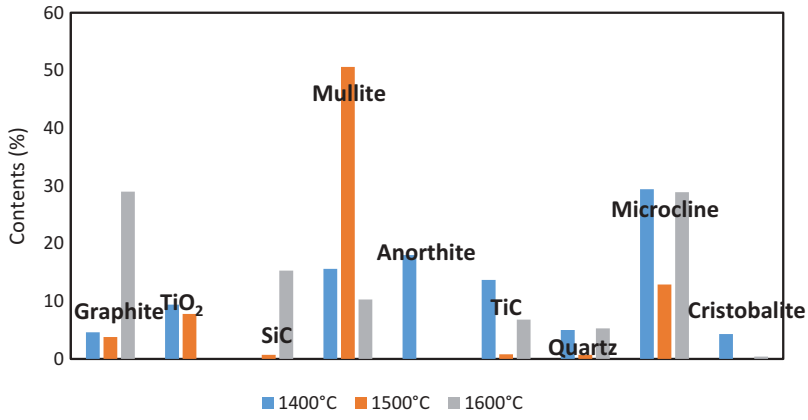

Figure 3. Effect of sintering temperature on the apparent porosity of the ceramic samples.

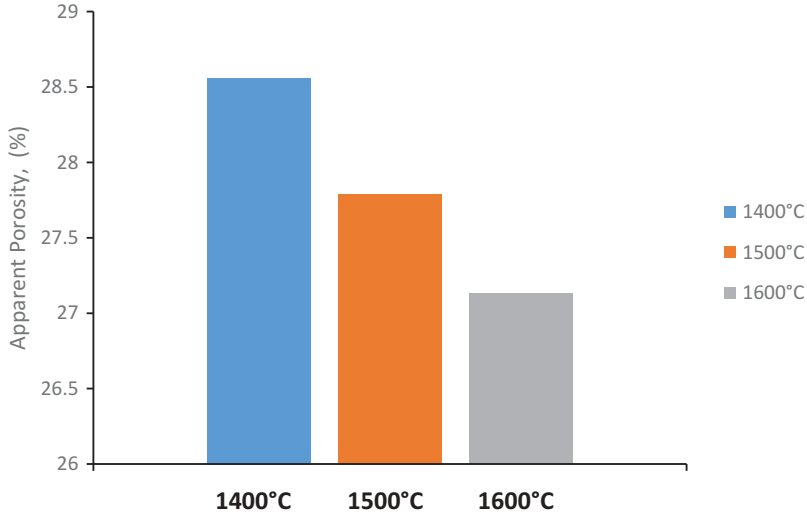

Figure 4. Effects of sintering temperature of the bulk density of the ceramic samples.

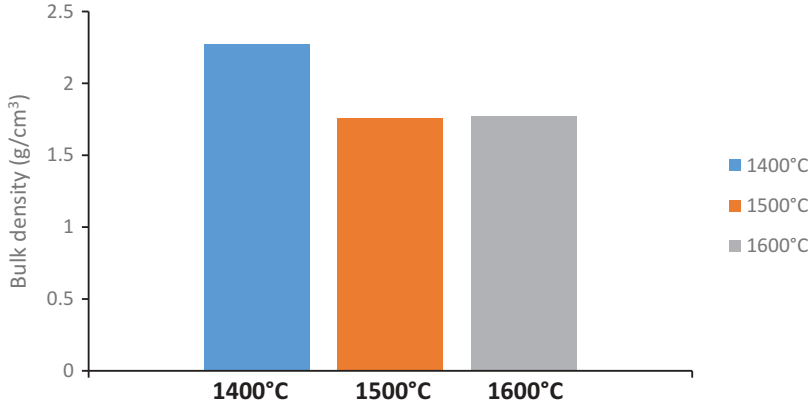

1400°C the phases present in the sample are 4.6% graphite, 9.4% titania, 15.6% mullite, 18.0% anorthite, 13.7% titanium carbide, 5.0% quartz, 29.4% microcline and 4.3% cristobalite. From Table 1, the raw materials from which the sample is constituted composed of 35% kaolin, 25% Ifon clay, 30% graphite, 5% SiC and 5% titania. It has been reported that when kaolinite (a constituent of kaolin clay) is subjected to firing at high temperature, it undergoes various phase changes from kaolinite through dehydroxylation to metakaolinite at around 420° to 660°C (Qiu, Jiang, Li, Fan, &

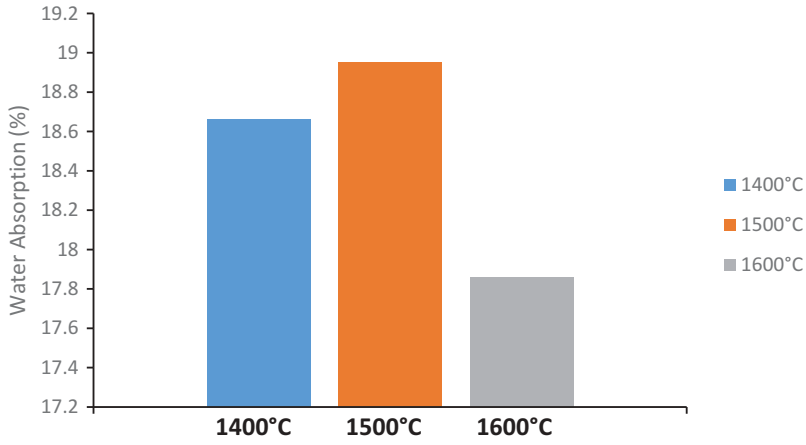

Figure 5. Effects of sintering temperature on the water absorption of the ceramic samples.

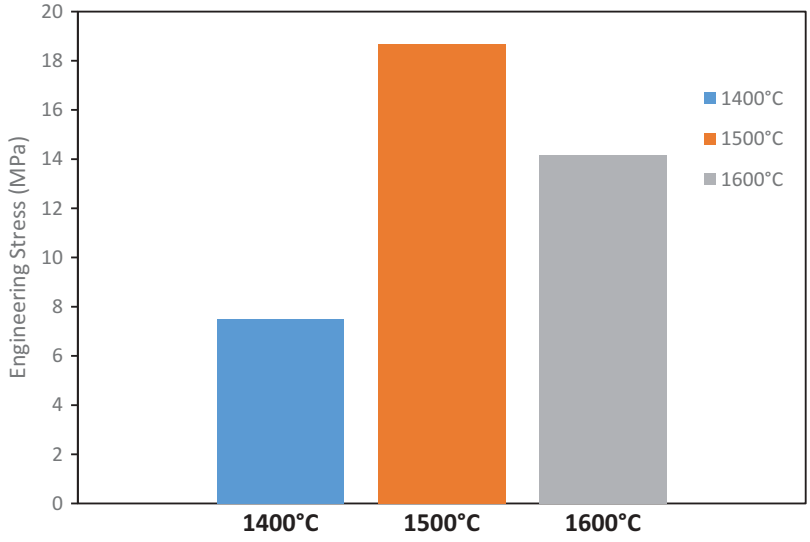

Figure 6. Effects of sintering temperature on the engineering compression stress of the ceramic samples.

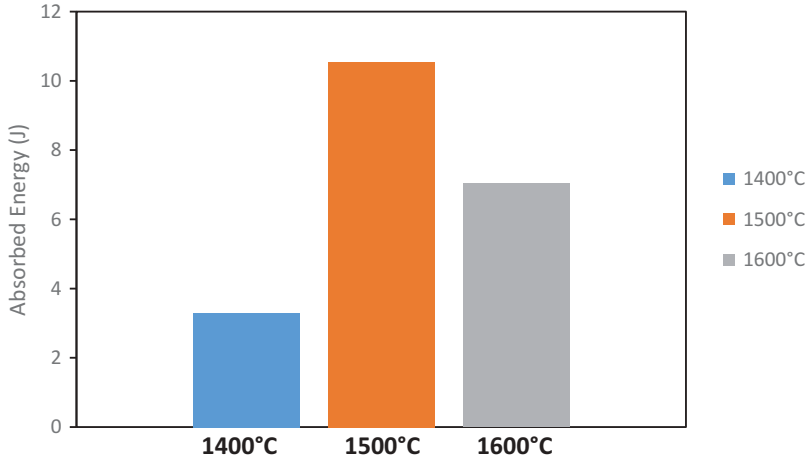

Figure 7. Effects of sintering temperature on the absorbed energy of the ceramic samples.

Huang, 2014). Furthermore, metakaolinite undergoes decomposition to amorphous silica and α-Al_2O_3 type spinel at around 900°C. As the sintering temperature increases, the spinel and silica recrystallizes to mullite above 1,100°C. However, some other researchers have reported that

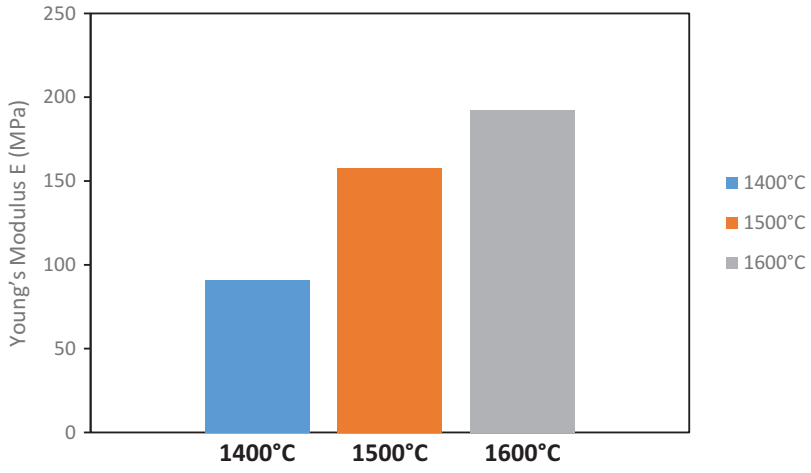

Figure 8. Effects of sintering temperature on Young's modulus of the ceramic samples.

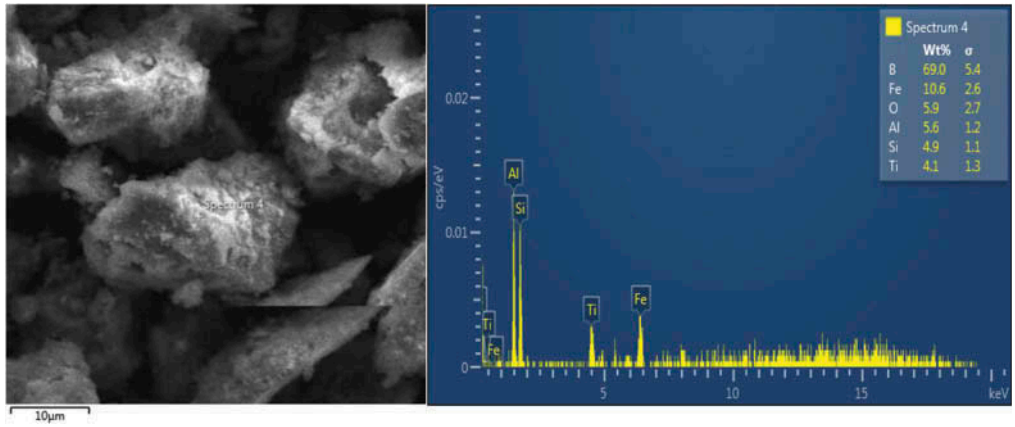

Figure 9. SEM images of sample DT1; showing secondary electron and backscattered images with EDS.

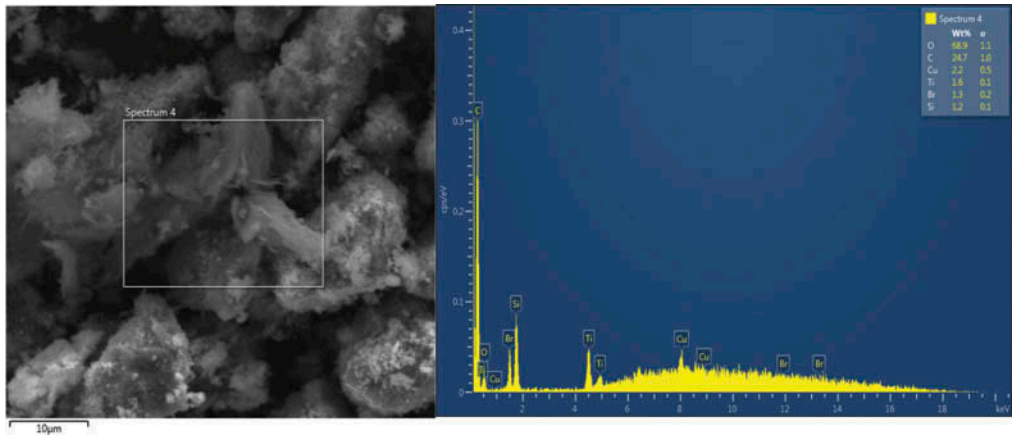

Figure 10. SEM images with EDS of sample DT2.

mullite begins to form with excess silica at a temperature above 900°C and continues till around 1,000°C (Aramide, 2012a; Srikrishna et al., 1990). This explains the origin of the mullite in the samples. However, the presence of anorthite and microcline could be attributed to the Ifon clay which has been reported to contain feldspar (Aramide, 2012b). Furthermore, Aramide (Aramide, 2015), reported his findings when he fired samples made from Ifon clay at temperatures between 800° and 1,200°C. He discovered that the major phases formed in the samples were quartz,

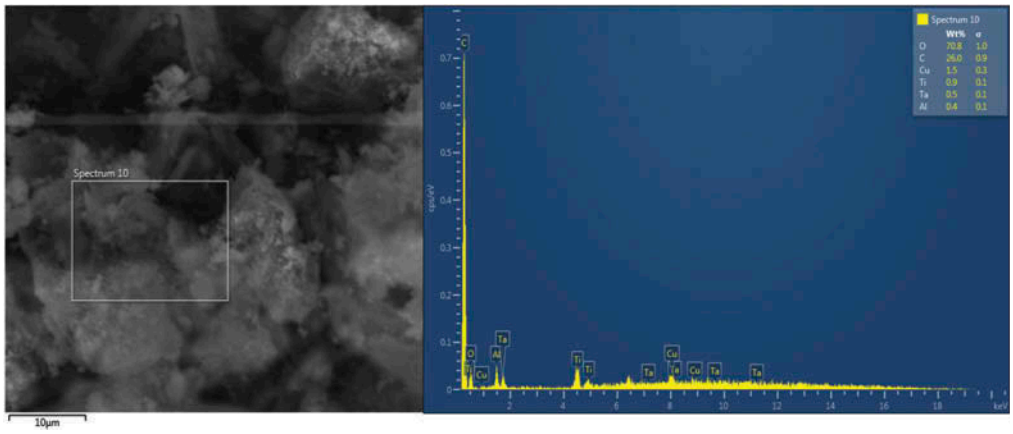

Figure 11. SEM images with EDS of sample DT3.

microcline and anorthite. This explains the origin of microcline and anorthite in the samples (Gridi-Bennadji, Beneu, Laval, & Blanchart, 2008; Gridi-Bennadji, Chateigner, Di Vita, & Blanchart, 2009).

However, as the sintering temperature was increased to 1,500°C, the amount of graphite in the sample is observed to reduce to 3.8%. Further increase in the sintering temperature (to 1,600°C) is observed to result in a sharp increase the amount of the graphite content to 29%. Moreover, the amount of titania in the sample is observed to slightly reduce to 7.8% as the sintering temperature is raised to 1,500°C. Beyond this temperature, the titania content is observed to reduce to 0% at 1600°C. It can be equally observed that at 1,400°C, no trace of silicon carbide was seen in the sample (even though about 5% SiC was part of the materials used in making the sample). It can be explained that the SiC added as part of the constituent in making the sample was oxidized to silica and carbon dioxide as reported by Roy *et al.* (Roy, Chandra, Das, & Maitra, 2014) who reported that silicon carbide undergoes active or passive mode of oxidation depending on the oxygen concentration (Callister, 2007) during which silica is liberated. This partly explains the origin of 5.0% quartz and 4.3% cristobalite (which are forms of silica). Furthermore, the initial 15.6% mullite in the sample at 1400°C is observed to increase to 50.6% with an increase in the sintering temperature to 1500°C. Further increase in the sintering temperature to 1600°C resulted in the amount of mullite being reduce to 10.3%. The 13.7% TiC observed in the sample at 1400°C could be said to be contributory to none existence of SiC in the sample at that temperature. It can be inferred that the TiO_2 reacted with the SiC to form TiC and SiO_2. As the sintering temperature is raised to 1,500°C, the amount of TiC is observed to reduce to 0.8% and then to increase to 6.8% when the sintering temperature was raised to 1,600°C.

Furthermore, at 1,400°C the anorthite content of the sample is observed to be 18.0%, as the sintering temperature was increased through 1500° to 1600°C the amount of anorthite in the sample was observed to reduce to 0%. It could be said that the presence of titania does not favour the stability of anorthite beyond 1,400°C. However, the initial 29.4% microcline content of the sample at 1,400°C is observed to reduce to 12.9% when the sintering temperature was raised to 1,500°C. Further, increased in the sintering temperature of the sample resulted in the amount of the microcline being increased to 28.9% at 1,600°C.

3.2. Effects of sintering temperature on the physical properties of the sintered ceramic samples

Figures 3–5 and Table 3 show the effects of sintering temperature and additives on the physical properties of the sintered ceramic samples.

3.2.1. Apparent porosity

The effects of sintering temperature on the apparent porosity of the sintered ceramic samples is depicted in Figure 3. From the figure can be observed that the apparent porosity of sample D reduced with increased sintering temperature from 1,400°C through 1,500°C and then to 1,600°C.

This is clearly seen in Figures 9, 10 and 11 which show the secondary electron images, and the EDS data of the samples. From Figure 9, it can be observed that the pore sizes and bigger (in sample DT1) than those in Figures 10 and 11 (samples DT2 and DT3). This relationship of porosity with sintering temperature is expected; because when ceramic is being sintered, the pores are closed up increasing the bulk density and reducing the porosity of the samples (Callister, 2007; Gridi-Bennadji et al., 2009).

However, it is established in the literature that although graphite is a refractory material, it does have a set-back of high-temperature oxidation at a temperature beyond 900°C (Aramide & Akintunde, 2017b; Zhang, Wang, & Chen, 2006). The graphite particles will be oxidized with increased sintering temperature, leaving voids within the ceramic material, thereby increasing the apparent porosity of the samples with increased sintering temperature. Why then does sample D has to behave differently? This can only be explained by looking at the other raw materials from which the samples were produced. Aramide and Akintunde (Aramide & Akintunde, 2017b) reported how about 4% SiC did impart high-temperature oxidation resistance to some graphite-based ceramic sample. Since 5% SiC is only 1% more than what they reported, it could be inferred that the 5% SiC did impart some level of oxidation resistance on the sample D. This is why its apparent porosity did reduce with increased sintering temperature. As explained earlier, the silica (quartz and cristobalite) formed during the reaction of TiO_2 with SiC filled up the pores in the samples thereby reducing the porosity with increased sintering temperature.

3.2.2. Bulk density

Figure 4 shows the effects of sintering temperature on the bulk density of the sintered ceramic samples. From the figure, it can be observed that the bulk density of the sample D was initially observed to be 2.271 g/cm^3 at 1,400°C, it reduced to 1.753 g/cm^3 as the sintering temperature was raised to 1500°C. Further, increase in the sintering temperature is observed to slightly raise the bulk density of the sample to 1.771 g/cm^3. Comparing this with the previous section, it is expected that the bulk density of the sample should increase with increased sintering temperature because its porosity reduced with increased sintering temperature (Aramide, 2012a; Aramide et al., 2017). The explanation that could be given for the reduction in bulk density with increased sintering temperature is that at 1,400°C it contained 13.7% TiC and 9.4% titania (Figure 2 and Table 3). These carbide and oxide have densities of 4.93 and 4.23 g/cm^3, respectively. The density of the sample reduced at 1,500°C because the content of TiC in it reduced to 0.8% while that of TiO_2 reduced to 7.8%. Further increase in the sintering temperature to 1,600°C lead to the content of the TiC in the sample to increase to 6.8% (which accounts for the slight increase in the bulk density) and TiO_2 reduced to 0%.

3.2.3. Water absorption

Figure 5 shows the effects of sintering temperature on the water absorption of the sintered graphite based ceramics samples. From the figure, it can be observed that water absorption of the sample was initially 18.66% at 1,400°C. When the sintering temperature was raised to 1,500°C the water absorption slightly increased to 18.95%, further increase in the sintering temperature resulted in the water absorption being reduced to 17.86%. The initial increase in the water absorption of the sample as the sintering temperature was raised from 1,400°C to 1,500°C implies that the open pores of the sample increased even though the porosity of the sample reduced with the range of the sintering temperature as was earlier discussed in Figure 3. Further increase in the sintering temperature to 1,600°C more of the open pores were closed up.

3.3. Effects of sintering temperature and additives on the mechanical properties of the sintered ceramic samples

Figures 6–8 and Table 3 show the effects of sintering temperature and additives on the various mechanical properties of the ceramic samples under consideration.

3.3.1. Cold crushing strength (engineering stress)

Figure 6 shows the effects of sintering temperature and additives on the engineering stress of the samples being considered. From the figure the engineering stress of the sample is observed to be initially 7.481 MPa at 1,400°C, it is increased to its maximum of 18.7 MPa as the sintering temperature was raised to 1,500°C. Further increase in the sintering temperature to 1,600°C is observed to lead to a reduction in the engineering stress of the sample to 14.168 MPa. Comparing this with what is earlier observed in Figure 3, at 1,400°C it is expected that the engineering stress of the sample will be the least, since it has the highest porosity.

The more porous material is the less its loadbearing ability (Norton, 1968). This explains why the cold crushing strength (engineering stress) of the sample sintered at 1400°C is the lowest. However, an anomaly is observed in the values of the engineering stress of the samples sintered at 1500°C and 1600°C: Judging from their apparent porosity values as earlier discussed, it is expected that the value of the engineering stress of the sample sintered at 1600°C will be the highest. But that was not the case, the explanation that could be given to this can be inferred from Figure 2 and Table 2 earlier discussed. Looking at Figure 2 and Table 2, it will be observed that the sample that was sintered at 1,500°C contains 50.6% mullite while the one that was sintered at 1,600°C contains only 10.3% mullite. The higher content of mullite in the sample sintered at 1,500°C reinforced it better than the one that was sintered at 1,600°C, hence it possesses higher engineering stress (Silvestre et al., 2015).

Moreover, from Figure 4, the sample that was sintered at 1,400°C is observed to have the highest bulk density. Based on this, it would be expected that it will possess the highest load-bearing capacity (engineering stress value). But in reality, it has the least value of engineering stress! The reason for this is the combined effect of its high porosity and low content of mullite. The sample that was sintered at 1,600°C has a value of engineering stress greater than that of the sample sintered at 1,400°C because it is the least porous of all the samples and it contained 10.3% mullite which is not much different from the content of 15.6% mullite for sample sintered at 1,400°C.

3.3.2. Absorbed energy

Figure 7 shows the effects of sintering temperature and additives on the absorbed energy of the sintered ceramic samples. From the figure, the sample is observed to have a value of 3.291 J for absorbed energy at 1,400°C, it is observed to increase sharply to about 10.541 J when the sintering temperature of the ceramic sample is raised to 1,500°C. It however reduced to about 7.043 J with further increase in the sintering temperature of the sample to 1,600°C. The relationship between the absorbed energy of the sample and the sintering temperature is observed to follow the same trend followed by the engineering stress of the sample with increased sintering temperature. The same explanation given in the previous section is applicable to this behaviour. The sample with more reinforcement is more toughened than the sample with less reinforcement. Both the phases present in the samples and their porosity have an influence on the engineering stress and absorbed energy of the samples.

3.3.3. Young's modulus of elasticity

Figure 8 shows the effects of sintering temperature and additives on Young's modulus of the samples. From the figure, it is observed that Young's modulus of the sample increased with increased sintering temperature. At 1,400°C, it is observed that the Young's modulus of the sample was 90.8042 MPa, it, however, increased to 157.5683 MPa as the sintering temperature was increased to 1,500°C. Further increase in the sintering temperature of the sample to 1,600°C is observed to lead to an increase in Young's modulus of the sample to 192.5311 MPa. Comparing Figure 8 with Figure 3, it will be observed that when the porosity of the samples reduced with sintering temperature Young's modulus of the sample increased with increased sintering temperature. Young's modulus is the measure of the rigidity of the sample; for a sample to be more rigid, it has to be less porous.

4. Conclusions

The addition of TiO_2 and SiC in the sample lead to the formation of TiC in the sample at 1400°C and 1600°C. This takes place through high-temperature solid-state reaction (reaction sintering) of TiO_2 and SiC. This also contributes to the reduction in the apparent porosity of the sample with increased sintering temperature. The presence of titania in the sample does not favour the stability of anorthite beyond 1,400°C. The formation of 50.6% mullite in the sample at 1,500°C made it have the highest cold crushing strength and absorbed energy. Young's modulus of the sample increased with increased sintering temperature. The sample sintered at 1,500°C is considered optimum.

Acknowledgements
The financial assistance of The World Academy of Science (TWAS) in collaboration with the National Research Foundation (NRF) towards this research is hereby acknowledged. Opinions expressed and conclusions arrived at, are those of the authors and are not necessarily to be attributed to TWAS and NRF. A.A.A. acknowledged Landmark University for their support.

Funding
This work was supported by the National Research Foundation of South Africa [105555].

Author details
Fatai Olufemi Aramide[1,2]
E-mail: foaramide@futa.edu.ng
E-mail: aramidefo@tut.ac.za
O. D. Adepoju[1]
E-mail: Sholapoju@gmail.com
Adeolu Adesoji Adediran[3]
E-mail: adediran.adeolu@lmu.edu.ng
ORCID ID: http://orcid.org/0000-0001-9457-1071
Abimbola Patricia Popoola[2]
E-mail: PopoolaAPI@tut.ac.za
[1] Department of Metallurgical and Materials Engineering, Federal University of Technology, P.M.B. 704, Akure, Nigeria.
[2] Department of Chemical, Metallurgical and Materials Engineering, Tshwane University of Technology, Staatsartillerie Road, Pretoria West, South Africa.
[3] Department of Mechanical Engineering, Landmark University, Omu-Aran, PMB 1001, Kwara State, Nigeria.

Citation information
Cite this article as: Studies on the combined effects of titania and silicon carbide on the phase developments and properties of carbon-clay based ceramic composite, Fatai Olufemi Aramide, O. D. Adepoju, Adeolu Adesoji Adediran & Abimbola Patricia Popoola, *Cogent Engineering* (2019), 6: 1584938.

References

Aramide, F. O. (2012a). Production and characterization of porous insulating fired bricks from ifon clay with varied sawdust admixture. *Journal of Minerals and Materials Characterization and Engineering*, *11*(10), 970-975.

Aramide, F. O. (2012b). Effect of firing temperature on mechanical properties of fired masonry bricks produced from ipetumodu clay. *Leonardo Journal of Science*, *11*(21), 70–82.

Aramide, F. O. (2015). Effects of sintering temperature on the phase developments and mechanical properties Ifon clay. *Leonardo Journal of Science*, *14*(26), 67–82.

Aramide, F. O., & Akintunde, I. B. (2017a). Effects of silicon carbide and sintering temperature on the properties of sintered mullite-carbon composite synthesized from okpella kaolin. *Acta Technica Corviniensis: Bulletin of Engineering*, *10*(3), 99–106.

Aramide, F. O., & Akintunde, I. B. (2017b). Effects of silicon carbide on the phase developments in mullite-carbon ceramic composite. *Leonardo Electronic Journal of Practices and Technologies*, *16*(31), 45–58.

Aramide, F. O., Akintunde, I. B., & Oyetunji, A. (2016). Insitu synthesis and characterization of mullite-carbon refractory ceramic composite from okpella kaolin and graphite. *Usak University Journal of Material Sciences*, *5*, 25–42. doi:10.12748/uujms.2017.39

Aramide, F. O., Akintunde, I. B., & Popoola, P. A. (2017). Effects of titania and sintering temperature on the phase development and properties of sintered mullite-carbon composite synthesized from okpella kaolin. *Acta Technica Corviniensis: Bulletin of Engineering*, *10*(4), 121–130.

Aramide, F. O., Alaneme, K. K., Olubambi, P. A., & Borode, J. O. (2014). Effects of 0.2Y-9.8ZrO_2 addition on the mechanical properties and phase development of sintered ceramic produced from Ipetumodu clay. *ANNALS of Faculty Engineering Hunedoara – International Journal of Engineering (Stevenage).*, *7* (4), 343–352.

Aramide, F. O., & Popoola, P. A. (2017). Effects of niobium oxide additive on the phase development and physico-mechanical properties of zirconia-clay ceramics composite. *Journal of Ceramic Processing Research*, *18*(8), 560–568.

ASTM C133 – 97. (2015). *Standard test methods for cold crushing strength and modulus of rupture of refractories*. West Conshohocken, PA: ASTM International.

Badiee, H., Ebadzadeh, T., & Golestani-Fard, F. (2001). The effect of additives on mullitization of Iranian and alusite. In *44th International Colloquium on Refractories* (pp. 126–130). Achen.

Callister, W. D. (2007). *Materials science and engineering: An introduction*. New York, NY: John Wiley & Sons.

Chandra, D., Das, G. C., Sengupta, U., & Maitra, S. (2013). Studies on the reaction sintered zirconia-mullite-alumina composites with titania as additive. *Cerâmica*, *59*, 487–494. doi:10.1590/S0366-69132013000300021

Ebadzadeh, T., & Ghasemi, E. (2002). Effect of TiO_2 addition on the stability of t-ZrO_2 in mullite-ZrO_2 composites prepared from various starting materials. *Ceramics International*, *28*, 447–450. doi:10.1016/S0272-8842(01)00117-1

Elgamouz, A., & Tijani, N. (2018). From a naturally occurring-clay mineral to the production of porous ceramic membranes. *Microporous and Mesoporous Materials*, *271*, 52–58. doi:10.1016/j.micromeso.2018.05.030

Gridi-Bennadji, F., Beneu, B., Laval, J. P., & Blanchart, P. (2008). Structural transformations of muscovite at high temperature by X-ray and neutron diffraction. *Applied Clay Science*, *38*(3–4), 259–267. doi:10.1016/j.clay.2007.03.003

Gridi-Bennadji, F., Chateigner, D., Di Vita, G., & Blanchart, P. (2009). Mechanical properties of textured ceramics from muscovite–Kaolinite alternate layers. *Journal of*

the European Ceramic Society, *29*, 2177–2184. doi:10.1016/j.jeurceramsoc.2009.01.004

Jayasankar, M., Hima, K. P., Ananthakumar, S., Mukundan, P., Pillai, P. K., & Warrier, K. G. K. (2010). Role of particle size of alumina on the formation of aluminium titanate as well as on sintering and microstructure development in Sol–Gel Alumina–Aluminium titanate composites. *Materials Chemistry and Physics*, *124*(1), 92–96. doi:10.1016/j.matchemphys.2010.05.072

Norton, F. H. (1968). *Refractories*. New York: McGraw-Hill.

Qiu, G., Jiang, T., Li, G., Fan, X., & Huang, Z. (2014). Activation and removal of silicon in kaolinite by thermo-chemical process. *Scandinavian Journal of Metallurgy*, *33*, 121-128.

Roy, J., Chandra, S., Das, S., & Maitra, S. (2014). Oxidation behaviour of silicon carbide. *A Reviews on Advanced Materials Science*, *38*, 29–39.

Silvestre, J., Silvestre, N., & de Brito, J. (2015). An overview on the improvement of mechanical properties of ceramics nanocomposites. *Journal of Nanomaterials*, *2015*, 1–13. doi:10.1155/2015/106494

Srikrishna, K., Thomas, G., Martinez, R., Corral, M. P., De Aza, S. D., & Moya, J. S. (1990). Kaolinite-mullite reaction series: A TEM study. *Journal of Materials Science*, *25*, 607–612. doi:10.1007/BF00714083

Zhang, H. Y., Wang, H. Q., & Chen, G. H. (2006). A new kind of conducting filler-graphite nano sheets. *Plastics*, *35* (4), 42–50.

Cogent Engineering **(ISSN: 2331-1916) is published by Cogent OA, part of Taylor & Francis Group.**

Publishing with Cogent OA ensures:

- Immediate, universal access to your article on publication
- High visibility and discoverability via the Cogent OA website as well as Taylor & Francis Online
- Download and citation statistics for your article
- Rapid online publication
- Input from, and dialog with, expert editors and editorial boards
- Retention of full copyright of your article
- Guaranteed legacy preservation of your article
- Discounts and waivers for authors in developing regions

Submit your manuscript to a Cogent OA journal at www.CogentOA.com